2018 SCEC Project Report * Project 18054

Seismic coupling on faults and correlations between geodetic data, seismicity and climatic signals

1. PROJECT GOALS

The main goals of the project include *(i) Examine correlations between strain rate seasonal fluctuations and earthquake cluster characteristics, (ii) Examine correlations between climatic changes and earthquake dynamics. A unique opportunity to conduct this natural experiment is provided by the recent drought of 2011-2014 and the El Nino of 2015-2016, and (iii) Assess the effect of non-stationary dynamics (geodetic, seismic) on estimation of seismic coupling.*

2. PROJECT METHODOLOGY

The key methodological part of the project, in relation to goals (i) and (ii), is estimation of the seasonal geodetic displacements and strain. Toward this goal, we consider time series between 2002.00 and 2018.25 from all continuous GPS stations in our study. The time series are obtained from the Nevada Geodetic Laboratory (Blewitt et al., 2018). We exclude those stations for which the time series are <2.5 year long, those within California's Great Valley where stations' seasonal signal is significantly different from those on adjacent bedrock (Amos et al., 2014), and those with significant transient signals not associated with known earthquakes. For those stations affected by a large nearby earthquake we exclude the part of the postseismic time series that exhibits transient motion. We analyze time series of the remaining 1,202 stations in the NA12 reference frame (Blewitt et al., 2013), which has removed daily continental-scale common mode displacements present in the IGS08 frame, including periodic loading signals related to hemisphere-scale water transport (Blewitt et al., 2001; Wu et al., 2003). Our analysis in NA12 therefore differs slightly with that in IGS08, because (1) the common mode signal is not exclusively periodic causing some slight differences in the estimation of the seasonal signal and (2) the continental-scale water loading cycle causes a small N-S oriented displacement gradient across our study area that yields a uniform strain of up to $\sim \pm 0.5 \times 10^{9}$ in fall and spring, respectively. Both aspects combined affect our analysis only in a very minor way. To each station's north, east, and vertical daily position time series, we fit a model that includes a rate, periodic signal, and offsets due to equipment changes and earthquake coseismic offsets. The periodic signal consists of an annual term and a semiannual term. We assume that the seasonal signal is constant over the period considered, which is generally an appropriate approximation. For clarity we present (horizontal) data and strain models that exclude 419 outlier stations but show in the supporting information nearly identical results for strain models based on all data.

The earthquake cluster analysis was performed according to the methods developed by the PI within previous SCEC projects (Zaliapin and Ben-Zion, 2013a,b)

3. PROJECT RESULTS

Summary of results: We performed several detailed studies using joint data on strain rates and seismicity in California, to document systematic coupled fluctuations of strain rates and selected seismic cluster statistics. The examined fluctuations are related to

precipitation-triggered fluctuations of the Earth surface, either seasonal (Sect. 2.1) or decadal (Sect. 2.2). We developed an improved version of earthquake declustered algorithm, which facilitates comprehensive examination of non-stationary dynamics of seismicity, e.g. non-homogeneous background rates (Sect. 2.3).

Project outcomes: The project results are presented in three peer-reviewed publications (one published, two in review), and multiple conference presentations.

3.1 Spatiotemporal Correlation Between Seasonal Variations in Seismicity and Horizontal Dilatational Strain in California [Kreemer and Zaliapin, *GRL*, 2018]

We extract significant spatially coherent strain variations from horizontal seasonal Global Positioning System (GPS) displacements in the American Southwest. The dilatational strain is largest in northern California with maximum margin-normal contraction and extension in spring and fall, respectively, consistent with the Earth's surface going down and up at those times. The northern California signal has a phase shift with respect to that in southern California and the Great Basin. For northern and southern California the proportion of larger earthquakes are in-phase and the aftershock productivity out of phase with the inferred Coulomb stress on the San Andreas fault system. The intensity of mainshocks is in-phase in the north as well but not in the south. This suggests that a seasonal increase in fault-normal extension may or may not trigger mainshocks, but when an earthquake happens at those times, they grow larger than they otherwise would, which would cause a larger stress reduction and result in fewer aftershocks. See Figure 1.

3.2 Drought-triggered magmatic inflation, crustal strain and seismicity near the Long Valley Caldera, Central Walker Lane [Hammond, Kreemer, Zaliapin, Blewitt, 2019, in review]

We use GPS data to show synchronization between the 2011-2016 drought cycle in California, accelerated uplift of the Sierra Nevada Mountains, and enhanced magmatic inflation of the Long Valley Caldera (LVC) magmatic system. The drought period coincided with faster uplift rate, changes in gravity seen in the Gravity Recovery and Climate Experiment (GRACE), and changes in standardized relative climate dryness index. These observations together suggest that the Sierra Nevada elevation is sensitive to changes in hydrological loading conditions which subsequently influences the LVC magmatic system. We use robust imaging of horizontal GPS velocities to derive time-variable shear and dilatational strain rates in a region with highly variable station distribution. The results show that the highest strain rates are near the eastern margin of the Sierra Nevada and western edge of the CWL passing directly through LVC. The drought period saw geographic shifts in the distribution in active shear strain in the central Walker Lane (CWL) more than 60 km from the LVC, delineating the minimum extent over which the active magmatic system effects the CWL tectonic environment. We analyze declustered seismicity data to show that locations with higher seismicity rates tend to be 1) areas with higher strain rates, and 2) areas in which strain rates increased during drought-enhanced inflation. We hypothesize that drought conditions reduce vertical surface mass loading which decreases pressure at depth in the LVC system, in turn enhances magmatic inflation, and drives horizontal elastic stress changes that redistribute active CWL strain and modulate seismicity.

3.3 Earthquake declustering using the nearest-neighbor approach in space-time-magnitude domain [Zaliapin and Ben-Zion, 2019, in review]

We introduce an algorithm for declustering earthquake catalogs based on the nearest-neighbor analysis of seismicity. The algorithm discriminates between background and clustered events and includes a random thinning that compares nearest-neighbor proximity of events with space-varying cluster threshold. The threshold is estimated using randomized-reshuffled catalogs that are stationary, have independent space and time components, and preserve the space distribution of the original catalog. Analysis of synthetic catalog produced by the Epidemic Type Aftershock Sequence model demonstrates that the algorithm correctly classifies over 80% of background and clustered events, correctly reconstructs the space-dependent background intensity, and shows high stability with respect to random realizations (over 75% of events have the same estimated type in over 90% of random realizations). The declustering algorithm is applied to the global NCEDC catalog with magnitudes $m \geq 4$ during 2000 – 2015; Southern California catalog with $m \geq 2.5$, 3.5 during 1981 – 2017; area around the Landers rupture zone with $m \geq 0.0$ during 1981 – 2015; and Parkfield segment of San Andreas fault with $m \geq 1.0$ during 1984 – 2014. The null hypotheses of stationarity and space-time independence are not rejected by several tests in the estimated background field of the global catalog and South California catalog with $m \geq 3.5$. Both hypotheses are rejected for catalogs with larger range of magnitudes. The deviations from the nulls are mainly due to temporal fluctuations of seismic intensity at given locations and switches of activity among fault segments, which can be traced back to the original catalogs. See Figure 2.

References:

1. Amos, C. B., Audet, P., Hammond, W. C., Bürgmann, R., Johanson, I. A., & Blewitt, G. (2014). Uplift and seismicity driven by groundwater depletion in central California. Nature, 509(7501), 483–486. https://doi.org/10.1038/nature13275
2. Blewitt, G., Hammond, W. C., & Kreemer, C. (2018). Harnessing the GPS data explosion for interdisciplinary science. EOS. https://doi.org/10.1029/2018ES005636
3. Blewitt, G., Kreemer, C., Hammond, W. C., & Goldfarb, J. M. (2013). Terrestrial reference frame NA12 for crustal deformation studies in North America. Journal of Geodynamics, 72, 11–24. https://doi.org/10.1016/j.jog.2013.08.004
4. Blewitt, G., Lavalée, D., Clarke, P., & Nurutdinov, K. (2001). A new global mode of Earth deformation: Seasonal cycle detected. Science, 294(5550), 2342–2345. https://doi.org/10.1126/science.1065328
5. Wu, X., Heflin, M. B., Ivins, E. R., Argus, D. F., & Webb, F. H. (2003). Large-scale global surface mass variations inferred from GPS measurements of load-induced deformation. Geophysical Research Letters, 30(14), 1742. https://doi.org/10.1029/2003GL017546
6. Zaliapin, I. and Y. Ben-Zion (2013a) Earthquake clusters in southern California, I: Identification and stability. *J. Geophys. Res*., 118, 2847-2864. doi: 10.1002/jgrb.50179
7. Zaliapin, I. and Y. Ben-Zion (2013b) Earthquake clusters in southern California, II: Classification and relation to physical properties of lithosphere. *J. Geophys. Res*., 118, 2865-2877. doi: 10.1002/jgrb.50178

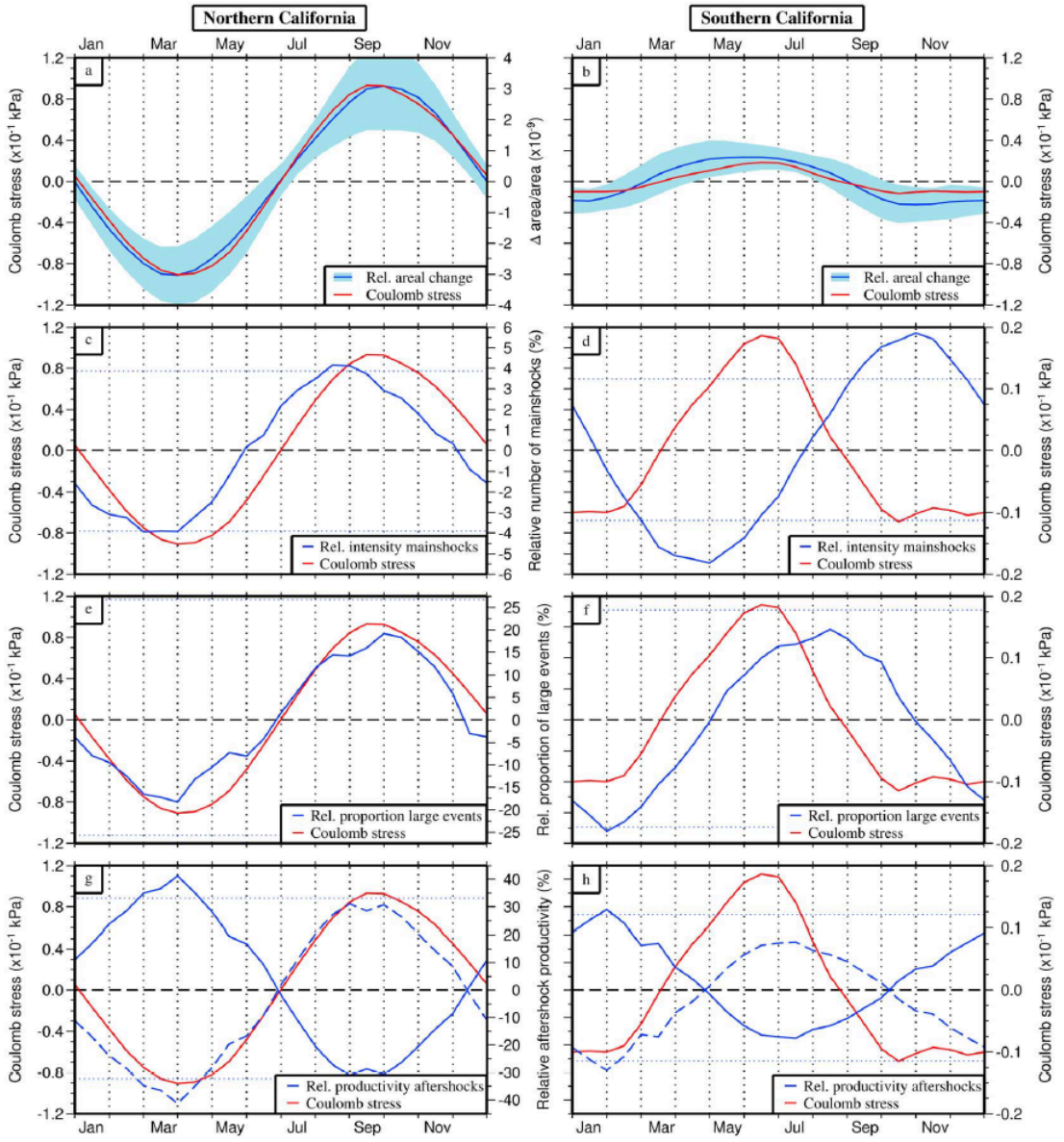

Figure 1: Left and right columns show results for polygons in northern and southern California, respectively. (a, b) Blue line shows seasonal variation in relative areal change (and the standard deviation therein). Red line indicates variation in Coulomb stress on a fault trending 35°W inferred from the strain tensor. Remaining panels (c–h) show in red the same Coulomb stress variations (with the results for southern California scaled up), blue lines show the examined statistic, temporally smoothed, and expressed relative to the median of all epochs (see section 3 and equation (1)) and thin dotted lines indicate the 5% and 95% empirical limits for each examined indicator, inferred by repeating the same analysis on multiple catalogs with reshuffled event times. (c, d) Number of mainshocks with $m \geq 2.5$. (e, f) Proportion of mainshocks with magnitude above or equal to 4.5 among mainshocks with magnitude above or equal to 3.5. (g, h) Aftershock productivity per cluster; see equation (2), and the negative value (dashed line). The axis description between the left and right panels applies to both panels.

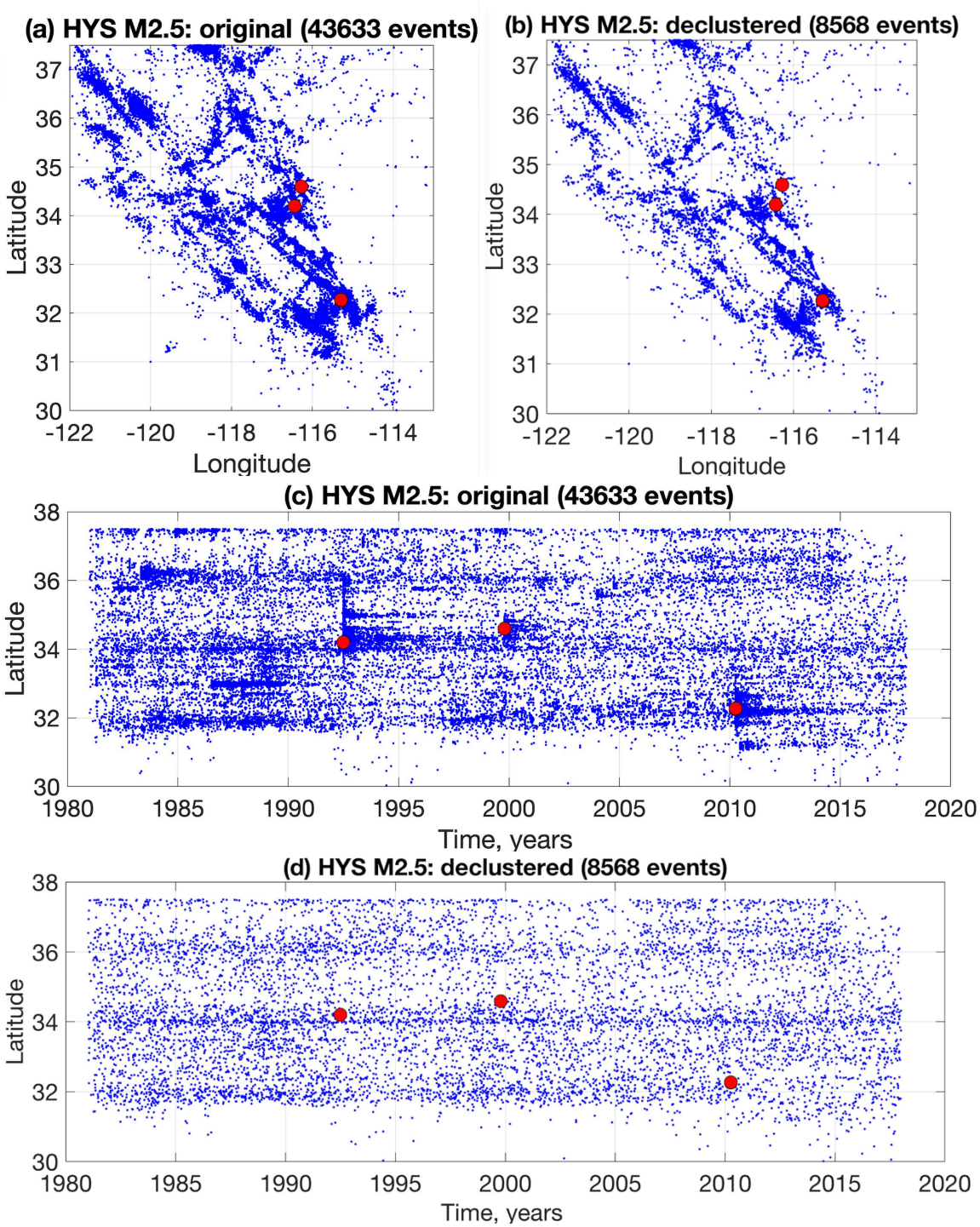

Figure 2: Declustering results for Southern California, $m \geq 2.5$, catalog of *Hauksson et al.* [2012] extended to 2017. Red circle marks the earthquakes with $m \geq 7$. (a) Original catalog, map view. (b) Declustered catalog, map view. (a) Original catalog, time-latitude sequence. (b) Declustered catalog, time-latitude sequence.

Project publications:

Published paper:

1. Kreemer, C. and I. Zaliapin (2018) Spatiotemporal Correlation Between Seasonal Variations in Seismicity and Horizontal Dilatational Strain in California. *Geophysical Research Letters*, *45*(18), 9559-9568. https://doi.org/10.1029/2018GL079536

Papers in review:

2. Hammond, W., C. Kreemer, I. Zaliapin, G. Blewitt (2019) Drought-triggered magmatic inflation, crustal strain and seismicity near the Long Valley Caldera, Central Walker Lane. In review.
3. Zaliapin, I. and Y. Ben-Zion (2019) Earthquake declustering using the nearest-neighbor approach in space-time-magnitude domain. In review.

Conference abstracts:

1. Cheng, Y., Y. Ben-Zion, and I. Zaliapin (2018) Informative space-time-magnitude-mechanism features of earthquakes in southern California. Abstract S41C-0534 presented at *2018 Fall Meeting of AGU, Washington D.C.*, December 10-14, 2018.
2. Kreemer, C. and I. Zaliapin (2018) Spatio-Temporal Correlation Between Seasonal Variations in Seismicity and Horizontal Dilatational Strain in California. Abstract G43A-07 presented at *2018 Fall Meeting of AGU, Washington D.C.*, December 10-14, 2018.
3. Zaliapin, I. and Y. Ben-Zion (2018) Earthquake clustering in relation to preparation of large events and seasonal strain signals. An invited talk presented at the *32nd IUGG Conference on Mathematical Geophysics*, Nizhny Novgorod, Russia, June 23-28, 2018.